

UV/O₃ assisted InP/Al₂O₃-Al₂O₃/Si low temperature die to wafer bonding

Anantha, P.; Tan, Chuan Seng

2015

Anantha, P., & Tan, C. S. (2015). UV/O₃ assisted InP/Al₂O₃-Al₂O₃/Si low temperature die to wafer bonding. *Microsystem technologies*, 21(5), 1015-1020.

<https://hdl.handle.net/10356/107400>

<https://doi.org/10.1007/s00542-015-2432-8>

© 2015 Springer-Verlag Berlin Heidelberg. This is the author created version of a work that has been peer reviewed and accepted for publication by Microsystem Technologies, Springer-Verlag Berlin Heidelberg. It incorporates referee's comments but changes resulting from the publishing process, such as copyediting, structural formatting, may not be reflected in this document. The published version is available at: [Article DOI: <http://dx.doi.org/10.1007/s00542-015-2432-8>].

Downloaded on 05 Apr 2024 09:01:08 SGT

UV/O₃ Assisted InP/Al₂O₃-Al₂O₃/Si Low Temperature Die to Wafer Bonding

P. Anantha and C.S Tan *

School of Electrical and Electronic Engineering, Nanyang Technological University, 50
Nanyang Avenue, Singapore 639798

*Email: tancs@ntu.edu.sg; Phone: +65-67905636

Abstract:

Direct bonding of InP dies to Si wafer at low temperature utilizing Al₂O₃ high-κ dielectric as the interfacial material for homogeneous bonding is reported. The bonding technique is assisted with a UV/Ozone exposure for surface activation and the activation time is optimized for the various intermediate layer thicknesses (5, 10, 20 nm). After the pre-bonding stage, annealing is carried out at 300 °C for 3 hrs. A bonding interface with minimal interfacial voids is reported for low intermediate layer thickness. The bonding interfaces are examined and a homogeneously bonded interface is shown in the IR images as well as in the FIB micrographs. Additionally a heat transfer simulation is also carried out and the InP/Al₂O₃-Al₂O₃/Si bonded structure is shown to closely match the thermal characteristics of a direct bonding approach with no intermediate layer. A high quality bonding interface is revealed along with improved heat dissipation characteristic for Al₂O₃ interface. Therefore, Al₂O₃ proves to be an advantageous candidate for its use in potential Si photonic integrated circuits application.

Introduction

A variety of materials such as metallic intermediates (Tsau *et al.* 2004; Tan and Reif 2005), and polymeric materials (Niklaus *et al.* 2006) have been utilized to achieve wafer bonding for 3D integration of circuit applications. The use of intermediate layers is specially required for the bonding of III-V materials onto Si due the lattice mismatch (Pasquariello and Hjort 2002). In this case, a number of dielectric materials are being investigated for their use as intermediate layers assisting in bonding of III-V materials onto Si at low temperature, for various potential applications in photonic integrated circuits (Pasquariello *et al.* 2001; Liang *et al.* 2009; Liang *et al.* 2010). The use of Al_2O_3 , TiO_2 and HfO_2 high- κ dielectrics has been reported to improve the bond strength in PE-TEOS oxide bonding (Chong and Tan 2009). In most studies, SiO_2 has been the most commonly used intermediate layer for bonding demonstrating improved performance in its use in optical devices (Ben Bakir *et al.* 2006; Ben Bakir *et al.* 2011). In consideration of the reported improved diffusion barrier layer properties and thermal properties reported (Fan *et al.* 2013) upon utilizing Al_2O_3 as the intermediate layer, its use is investigated further in this work.

In this study Al_2O_3 is utilized as the intermediate layer for the low temperature bonding of InP dies onto Si wafer. A homogeneous type of bonding is employed in this study by depositing intermediate layers of uniform thickness onto both the die and wafer surfaces. As a hydrophilic bonding is desirable for fusion bonding in this study, the surface activation is carried out using UV/Ozone technique in ambient air. This technique provides a simple operating procedure and thus proves to cost efficient. Furthermore, a thermal simulative study is also carried out validating the advantages provided by the Al_2O_3 intermediate layer.

Experimental Methodology

Firstly, both silicon wafer and InP dies are cleaned to eliminate surface contaminants. A conventional Piranha clean (H_2O_2 and H_2SO_4) is employed for Si wafer and the InP dies are rinsed using acetone, IPA and ammonia hydroxide (NH_4OH). The subsequent step of atomic layer deposition of Al_2O_3 film is carried out at 250°C to obtain 5, 10, and 20 nm thick of the intermediate layer, respectively. The surface activation process critical to the current study is carried out using a UV/Ozone system. This process aids in preparing a hydrophilic surface suitable for direct bonding technique. In addition, the method is also capable of resulting in a surface free of organic contaminants (Gösele and Tong 1998). The optimized activation time for varying Al_2O_3 film thickness is shown in Figure 1 (8 minutes for 10 nm, and 6 minutes for 5 nm thickness, respectively). The surface roughness and water contact angle values measured are used to optimize the activation time.

Post activation the samples are rinsed using DI water, dried and brought into contact face to face in clean room ambient. This step is followed by maintaining the samples at 2 MPa of applied pressure for 2 hours. The 2 hours is the optimized pressure timing for the bonding of small dies. The final step involves the annealing of these bonded samples at 300°C for 3 hrs. The annealing process is known to substantially improve the wafer bonding strength (Gösele and Tong 1998).

Results and Discussion

In this section the experimental characterization results of bonded interface are discussed. In the next section, the thermal characteristics of the various bonding interfaces obtained using a simulative method is reported.

A. Characterization of the Bonding Interface

Bonded dies are first viewed under IR imaging to identify the presence of large interfacial voids. Reduced void densities are seen for dies activated for 6 and 8 minutes. These are also in agreement with the low surface roughness and improved hydrophilicity (low contact angle). The IR images obtained for the various dies are tabulated in Table I for 5 and 10 nm film thicknesses. The fringes formed at the bonding interface can be observed to be existent mostly at the die edges only. This is related to surface damages arisen during sample preparation and handling of the InP dies prior to bonding. Given the brittleness of the InP dies, chipping of the edges is common. This results in formation of tiny contaminants, which affect the bonding quality. Therefore small dies must be handled with caution and effective cleaning steps could be employed to reduce these effects and thus improve bonding quality. The optimized activation time are 6 or 8, as they aid in achieving a bonding interface with minimized interfacial voids (Table 1). In addition, these activation times also provide for a minimized surface roughness as compared to other activation times (Figure 1).

The bonded interface is further examined by observing under a Transmission Electron Microscope (TEM). The low and high magnification micrographs of the bonded interface are shown in Figure 2. The TEM samples were prepared using the Focused Ion Beam (FIB) technique. The TEM images have been taken from the bonded regions of the interface. The FIB sample is cut from these zones and their bonding interface is observed. The successful sample preparation implies the bond strength to be sufficiently strong. It is clearly seen that the bonded interface is well fused and the interfacial void density is minimal. The interface captured is bonded using 10 nm of Al_2O_3 as the intermediate layer.

Furthermore elemental mapping of the interface confirms minimal inter-diffusion at the homogeneously bonded interface (Figure 3). The color coding indicates the position of each of the element present in the first image shown on the left hand side, as seen in the image. The elements identified in the TEM image also assist in validating that Al_2O_3 provides efficient barrier layer properties (Hirvikorpi *et al.* 2011) along with acting as an efficient intermediate bonding layer. The bonding strength is also anticipated to be strong in this system, as an ionic type of bonding is present between the two Al_2O_3 layers. This type of bonding has also been reported among wafer-wafer bonding also utilizing Al_2O_3 as the intermediate layer (Chong and Tan 2011).

However in some samples the formation of interfacial voids was persistent. They were observed under the optical microscope and is shown in Figure 6. The top InP layer was etched away using wet chemical etching process (equal parts of H_3PO_4 : HCl : H_2O). InGaAs was the etch stop layer employed. The generation of these bubbles was due to the release of by-product gases during the hydrophilic bonding process. Thus the use of out-gassing channels for the removal of these by-product gases is essential to obtain a void-free interface. This can aid in improving the final device efficiency and also increase the bond strength due to the increase in bonding area.

B. Simulation of Thermal Characteristics at the Bonding Interface

The influence of utilizing different types of interfaces for bonding was investigated by finite element COMSOL simulation method. Three different systems utilizing (a) a direct bonding of InP to Si; (b) Al_2O_3 as the intermediate layer and (c) SiO_2 as the intermediate layer were

investigated. The model consists of InP (1 μm), Si (10 μm) and the intermediate layer thicknesses is varied from 2 to 30 nm. The thermal conductivities of the of the two intermediate layers were 30 $\text{WK}^{-1}\text{m}^{-1}$ (Al_2O_3) and 1.46 $\text{WK}^{-1}\text{m}^{-1}$ (SiO_2) and the bottom surface of the Si substrate was maintained at 25 $^\circ\text{C}$. The heat dissipation characteristics were simulated along the bonding interface when a heat flux of 10,000 W/cm^2 was applied. The results obtained across the three different interfaces are shown in Figure 5.

It can be observed that the heat dissipation characteristic of Al_2O_3 interface is very similar to the directly bonded interface. The SiO_2 interface, however, displays large thermal resistance and heat spreading through the bottom Si substrate is not effective. This is due the difference in thermal conductivity between the two interfacial layer materials. The characteristic of Al_2O_3 as the interfacial layer which does not significantly alter the heat dissipation characteristics of a direct bonding technique is advantageous. Hence, these properties of Al_2O_3 make it highly valuable as an intermediate layer for bonding. Furthermore, the thickness effect on the heat dissipation characteristics was also investigated and is shown in Figure 6. The intermediate layer thicknesses were varied from 2 to 50 nm (power density applied - 10,000 W/cm^2) and their change in temperature at the top surface was recorded and plotted. The use of Al_2O_3 hardly showed any difference in the highest temperature whereas SiO_2 displayed a 1.5 $^\circ\text{C}$ difference with increasing thickness. This result yet again confirms the efficient heat dissipation characteristic of Al_2O_3 .

Conclusion

InP and Si direct die to wafer bonding is carried out in room ambient followed by low temperature annealing. Al_2O_3 has been utilized as the interfacial layer to demonstrate a

homogeneous type of bonding. The bonding surfaces were activated using UV/Ozone technique to improve their surface hydrophilicity, thus assisting in the bonding process. A well bonded interface, homogeneous interface was revealed from the IR and TEM imaging techniques. In addition to these improved bonding qualities provided by Al_2O_3 , its thermal property was also tested from simulation. COMSOL studies indicated the intermediate layer to allow an improved heat dissipation interface. Therefore the advantages provided by Al_2O_3 have been discussed and an improved bonding of InP dies to Si is shown with potential applications in photonics.

Acknowledgement

This work was financially supported by the Agency for Science, Technology and Research (A*STAR) with a project #1122804038. Authors are grateful for the support and resources from the Silicon Technologies Center of Excellence (Si-COE). C.S. Tan is affiliated with NOVITAS (Nanoelectronics Centre of Excellence) at NTU.

References:

- Ben Bakir B, Descos A, Olivier N, et al. (2011) Electrically driven hybrid Si/III-V Fabry-Pérot lasers based on adiabatic mode transformers. *Opt Express* 19:10317–10325.
- Ben Bakir B, Seassal C, Letartre X, et al. (2006) Surface-emitting microlaser combining two-dimensional photonic crystal membrane and vertical Bragg mirror. *Appl Phys Lett* 88:081113–081113–3. doi: 10.1063/1.2172730
- Chong GY, Tan CS (2009) Low Temperature PE-TEOS Oxide Bonding Assisted by a Thin Layer of High- κ Dielectric. *Electrochem Solid-State Lett* 12:H408. doi: 10.1149/1.3207872
- Chong GY, Tan CS (2011) PE-TEOS Wafer Bonding Enhancement at Low Temperature with a High- κ Dielectric Capping Layer of Al₂O₃. *J Electrochem Soc* 158:H137. doi: 10.1149/1.3507291
- Fan J, Anantha P, Liu CY, et al. (2013) Thermal Characteristics of InP-Al₂O₃/Si Low Temperature Heterogeneous Direct Bonding for Photonic Device Integration. *ECS J Solid State Sci Technol* 2:N169–N174. doi: 10.1149/2.012309jss
- Gösele U, Tong Q-Y (1998) Semiconductor Wafer Bonding. *Annu Rev Mater Sci* 28:215–241. doi: 10.1146/annurev.matsci.28.1.215
- Hirvikorpi T, Vähä-Nissi M, Nikkola J, et al. (2011) Thin Al₂O₃ barrier coatings onto temperature-sensitive packaging materials by atomic layer deposition. *Surf Coat Technol* 205:5088–5092. doi: 10.1016/j.surfcoat.2011.05.017
- Liang D, Bowers JE, Oakley DC, et al. (2009) High-Quality 150 mm InP-to-Silicon Epitaxial Transfer for Silicon Photonic Integrated Circuits. *Electrochem Solid-State Lett* 12:H101. doi: 10.1149/1.3065994
- Liang D, Roelkens G, Baets R, Bowers JE (2010) Hybrid Integrated Platforms for Silicon Photonics. *Materials* 3:1782–1802. doi: 10.3390/ma3031782
- Niklaus F, Stemme G, Lu J-Q, Gutmann RJ (2006) Adhesive wafer bonding. *J Appl Phys* 99:031101. doi: 10.1063/1.2168512
- Pasquariello D, Camacho M, Hjort K, et al. (2001) Evaluation of InP-to-silicon heterobonding. *Mater Sci Eng B* 80:134–137. doi: 10.1016/S0921-5107(00)00626-7
- Pasquariello D, Hjort K (2002) Plasma-assisted InP-to-Si low temperature wafer bonding. *IEEE J Sel Top Quantum Electron* 8:118–131. doi: 10.1109/2944.991407
- Tan CS, Reif R (2005) Silicon Multilayer Stacking Based on Copper Wafer Bonding. *Electrochem Solid-State Lett* 8:G147–G149. doi: 10.1149/1.1904506
- Tsau CH, Spearing SM, Schmidt MA (2004) Characterization of wafer-level thermocompression bonds. *J Microelectromechanical Syst* 13:963–971. doi: 10.1109/JMEMS.2004.838393

Figure Captions:

Figure 1: AFM scans for 10 nm Al_2O_3 films deposited onto InP surfaces are shown with their corresponding contact angle measurements (inset), for activation times of 0, 6, 8 & 10 minutes.

Figure 2: (a) Low magnification TEM micrograph of the InP/ Al_2O_3 /Si bonded interface & (b) High resolution TEM image showing the homogeneously bonded interface using Al_2O_3 intermediate layer.

Figure 3: Elemental mapping at the bonded interface showing the various elemental presences and the layer stacking without interdiffusion.

Figure 4: Interfacial voids formed at the bonding interface of InP-Si, captured using optical microscope

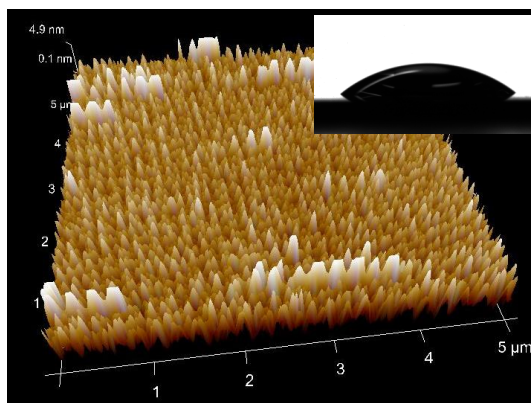
Figure 5: Temperature profile as seen from simulated bonded structures at varying bonding interfaces: (a) direct bonding InP and Si; (b) 50 nm Al_2O_3 as the intermediate layer; (c) 50 nm SiO_2 as the intermediate layer.

Figure 6: Varying thickness effect for (a) Al_2O_3 & SiO_2 on InP chip temperature simulated using a heat flux of $10,000 \text{ W/cm}^2$ (b) The thickness of Al_2O_3 is shown in a separate plot for clarity.

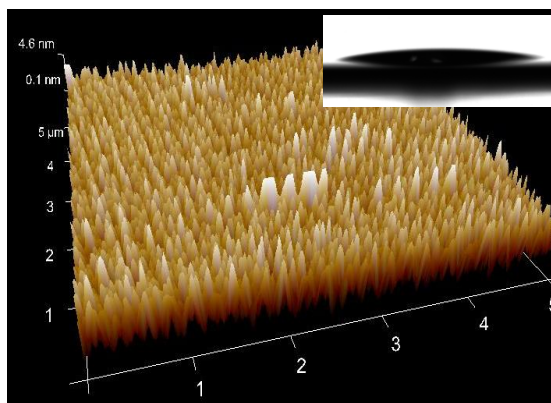
Table Caption:

Table 1: IR images of dies bonded after UV/Ozone activation for 6 and 8 minutes with 10 nm & 5 nm interfacial layer thicknesses.

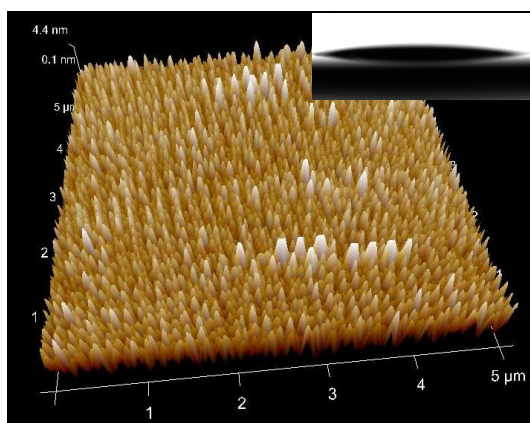
Figures:



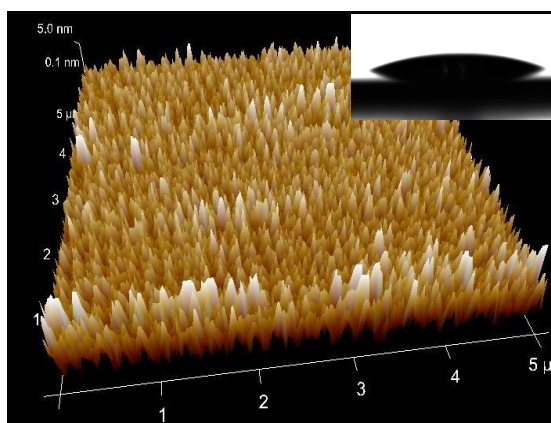
0 minutes: $\sim 43^\circ$; 1.65 nm (RMS)



6 minutes: $\sim 10.3^\circ$; 1.33 nm (RMS)



8 minutes: $\sim 6.9^\circ$; 1.4 nm (RMS)



10 minutes: $\sim 11.3^\circ$; 1.52 nm (RMS)

Figure 1

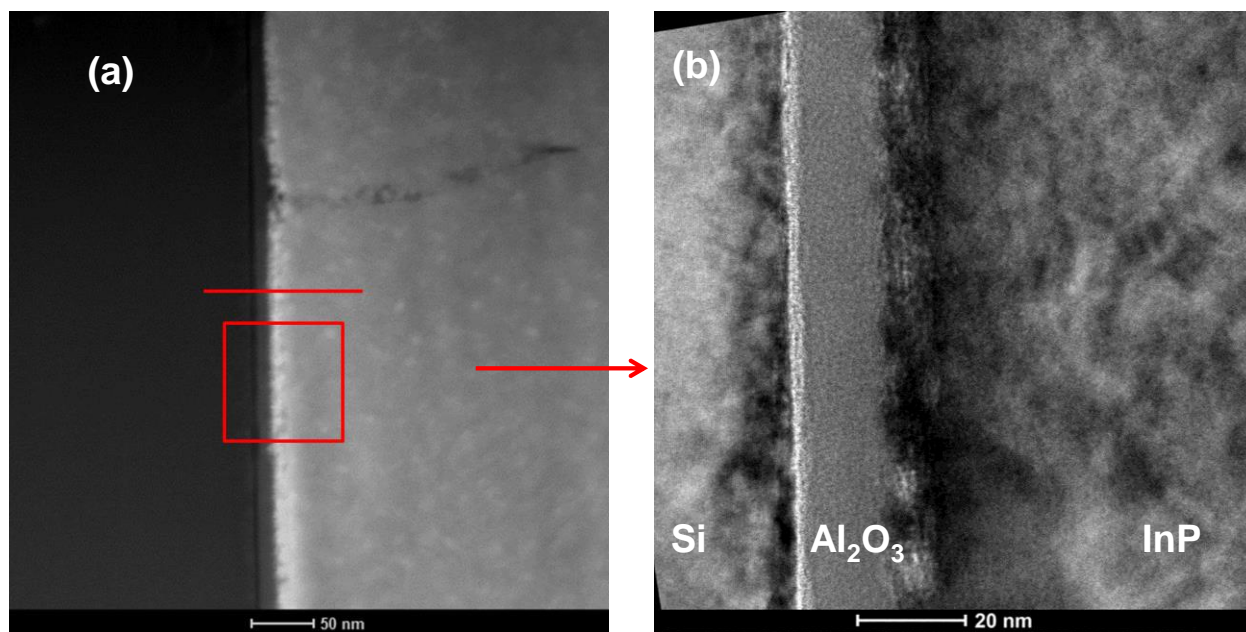


Figure 2

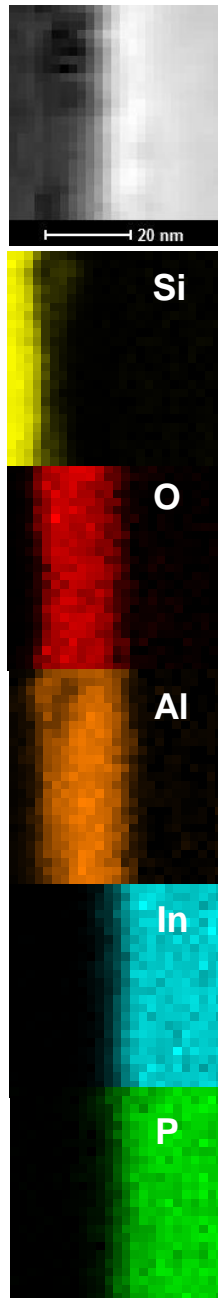


Figure 3

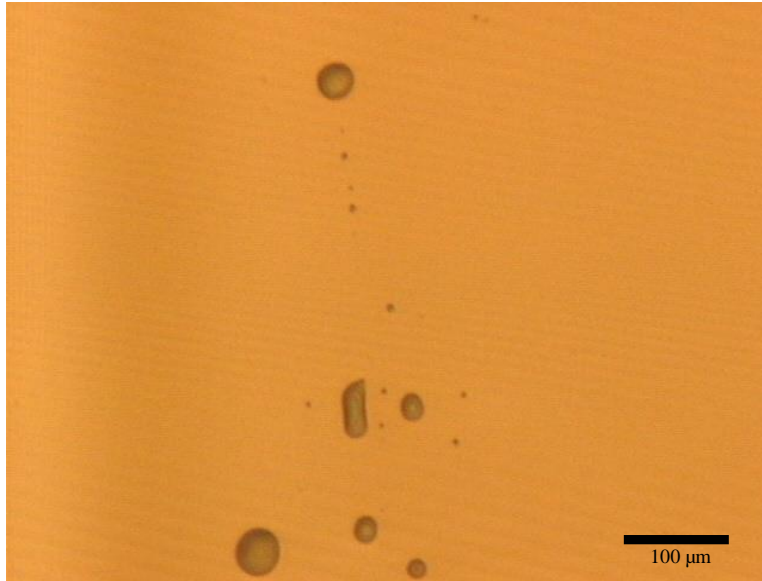


Figure 4

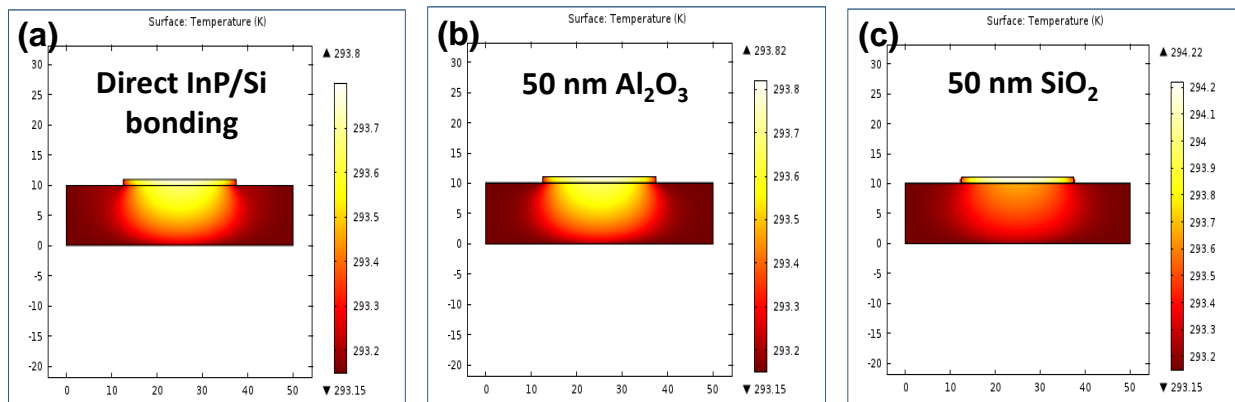


Figure 5

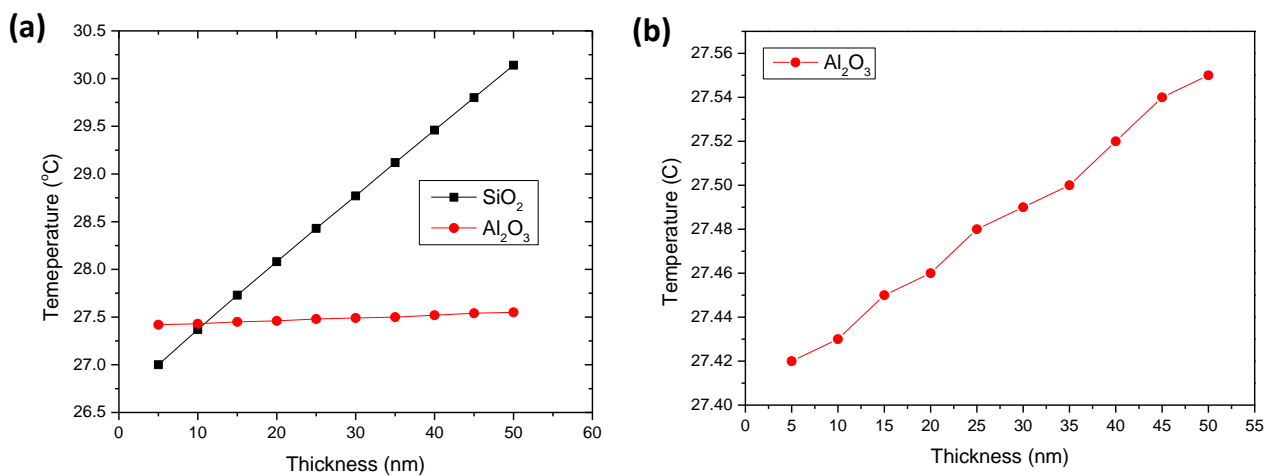




Figure 6

Table:

Table I

Activation Time	Thickness 10 nm	Thickness 5 nm
6 minutes		
8 minutes	